

# GEOMETRICAL DEGENERACY REMOVAL BY VIRTUAL DISTURBANCES

## *An Application to Surface Reconstruction from Point Slice Samples*

Oscar Ruiz

CAD CAM CAE Laboratory, EAFIT University, Medellin, Colombia

Eliana Vasquez<sup>1</sup>, Sebastian Peña<sup>2</sup>, Miguel Granados<sup>3</sup>

<sup>1</sup>Erasmus Universitaet, Nederlands

<sup>2</sup>Fraunhofer Inst. Comp. Graphics, Germany

<sup>3</sup>Max Planck Inst. Informatiks, Germany

**Keywords:** Geometric degeneracy, Voronoi diagram, Delaunay triangulation, surface reconstruction, slice point sample.

**Abstract:** In surface reconstruction from slice samples (typical in medical imaging, coordinate measurement machines, stereolithography, etc.) the available methods attack the geometrical and topological properties of the surface. Topological methods classify the transitions occurred in the 2-manifold between two consecutive slices  $i$  and  $i + 1$ . Geometrical methods synthesize the surface based on local proximity of the contours in consecutive slices. Superimposed 2D Voronoi Diagrams  $VD_i$  and  $VD_{i+1}$  for slices  $i$  and  $i + 1$ , respectively, present topological problems if, for example, a site of  $VD_i$  lies on an site or an edge of  $VD_{i+1}$ . The usual treatment of this problem in literature is to apply a geometrical disturbance to either  $VD_i$  or  $VD_{i+1}$ , thus eliminating the degeneracy. In contrast, this article presents the implementation of a method which identifies the degenerate situation, constructs un-instantiated topological constructs, choses a geometrical instantiation based on a virtual disturbance introduced to the actual configuration. The algorithm was successfully applied to remove non-manifold topologies produced by well known algorithms in surface reconstruction.

## 1 INTRODUCTION

Degenerate conditions in geometric algorithms have been dealt with different ways: (i) by stating the same problem in different spaces with better conditioning, (ii) by increasing the real computation precision, (iii) by relying on rational numbers, with no rounding errors, and (iv) by disturbing the input for the geometrical algorithms, while at the same time estimating the probability of respecting the original problem topology. Strategies (i) and (ii) have been extensively applied in Numerical Analysis, for example, by generating equivalent linear systems with better manipulation properties. Alternative (iii) has been investigated, for example in Computational Geometry Algorithm Library (Burnikel et al., 1999), with exact computation paradigms. Strategy (iv) has given probability bounds for alteration of Voronoi-Delaunay topology upon numerical disturbance of degenerate events (Funke et al., 2005). Virtual Perturbations have been used in other contexts (Edelsbrunner

and Mücke, 1990). It should be noticed that none of the mentioned strategies solves the degeneracy problem. Each is suited for a particular domain of problems.

The strategy presented here assumes the possibility of detecting the degenerate condition, and to create a finite number of topological configurations for the solution. The geometrical and topological objects created are not numerically instantiated, until the very end of the proposed scheme. The strategy presented here is clearly convenient when there is a finite number of topological configurations, which can be enumerated and distinguished.

The particular context in which this strategy is presented is the general problem of surface reconstruction, from planar samples. Particular steps of the Boissonat & Geiger algorithm (Boissonat, 1988; Geiger, 1993) have been changed in order to make them more robust (Ruiz et al., 2002; Ruiz et al., 2005). Section 2 gives the application context of the present work and reviews related literature. Section 3 de-

scribes the methodology applied and the procedures followed. Section 4 gives an account of the results, and section 5 concludes the article.

## 2 CONTEXT AND LITERATURE REVIEW

The scenario to apply the proposed algorithm for degeneracy control is the following: Consider a solid object  $B$ , whose boundary  $M = \partial B$  is a smooth 2-manifold or shell in  $R^3$ . Consider a set of parallel planes  $\Pi_i, i = 0, 1, 2, \dots$  sectioning  $M$ , and therefore producing traces of  $M$  which are Jordan curves  $\Gamma_{j,i}$  or contours drawn on the planes  $\Pi_i$ . Recovering  $M$  from the contour set boils down to recovering  $M_{i,i+1}$ , the portion of  $M$  contained between the planes  $\Pi_i$  and  $\Pi_{i+1}$ .

The algorithm proposed and implemented by Boissonat & Geiger in (Boissonat, 1988; Geiger, 1993) (called here **B+G**) builds tetrahedra filling the space between two consecutive sampling planes  $i$  and  $i + 1$ . B+G is a fairly fast and robust algorithm, originally presenting weaknesses that have been corrected by complementary works ((Ruiz et al., 2005)). The boolean union of such tetrahedra produces the portion of the solid contained between the planes  $i$  and  $i + 1$ . B+G basically uses local geometrical proximity between contours to construct the surface  $M_{i,i+1}$ . As a consequence, over-stretched surfaces may be generated joining contours on the planes  $i$  with those on plane  $i + 1$  which have little to do with each other in the global sense. This effect may be diminished by applying a 2D shape similarity (2DSS) algorithm (Ruiz et al., 2002; Ruiz et al., 2005). In B+G, the tetrahedra are built by projecting the Voronoi Diagram (VD) of the point set in level  $i, VD_i$ , onto  $VD_{i+1}$ , or vice versa. A degeneracy condition for B+G occurs when a Voronoi site of  $VD_i$  exactly lies on either a Voronoi site or a Voronoi edge of  $VD_{i+1}$ . Such a condition produces a non-manifold and self - intersection condition in the surface built by B+G. The work presented in this article corresponds to the application of late numerical instantiation of topological and geometrical objects to solve such a degeneracy.

### 2.1 Brief Review of the B+G Method

The B+G method divides the interior of the contours in triangles by creating the Delaunay Triangulation of the contour vertices (figures 2 and 3). After some processing, the Voronoi Diagrams belonging to the levels are used to create a planar graph named the Joint Voronoi Diagram (figure 4). This graph states how

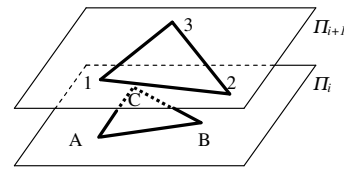


Figure 1: Original contours.

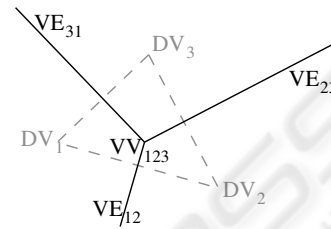


Figure 2: Delaunay Triangulation and Voronoi Diagram of the contours.

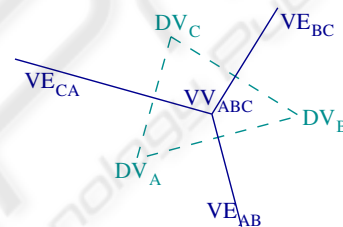


Figure 3: Delaunay Triangulation and Voronoi Diagram of the contours.

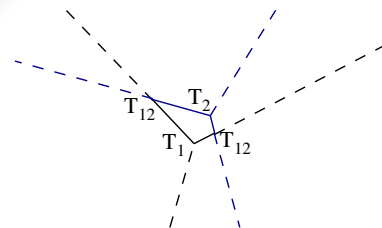


Figure 4: Delaunay Triangulation and Voronoi Diagram of the contours.

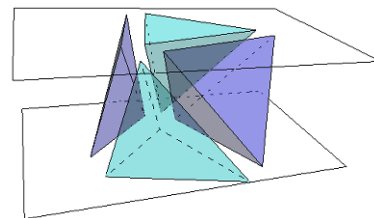


Figure 5: Related tetrahedrons.

the triangles in the levels are linked, by translating then to tetrahedrons (figure 5). Finally the triangles of the tetrahedrons facing the exterior are taken as the reconstructed surface.

### 3 IMPROVEMENTS ON THE B+G METHOD

The Polyhedral Surface Method, presented here in (Ruiz et al., 2005) is based on the B+G method. In the following discussion it will be shown that the B+G method may reconstruct incomplete surfaces and present non manifold situations. With our method the non manifold situations are minimized by preemptively considering special configurations of the Joint Voronoi Diagram (section 3.1).

#### 3.1 Special Cases in the Creation of the Joint Voronoi Diagram

The Joint Voronoi Diagram of two consecutive levels results from intersecting the orthogonal projections of their Voronoi Diagrams on a common plane. The Joint Voronoi Diagram is formed by three kinds of nodes:  $T_1$ ,  $T_2$  and  $T_{12}$ . The  $T_1$  and  $T_2$  nodes correspond to the Voronoi vertices belonging to the Voronoi Diagram on levels  $i$  or  $i+1$ . The  $T_{12}$  nodes correspond to the intersection of Voronoi edges, coming from levels  $i$  or  $i+1$ .

Every node in the graph corresponds to a tetrahedron, and the union of all these tetrahedrons forms the 3D Delaunay Diagram of the contour points  $P$  on both levels  $i$  and  $i+1$ . Because the tetrahedrons that are translated from the graph are Delaunay tetrahedrons, they satisfy the “empty-sphere” condition, namely is, the sphere that circumscribes the tetrahedron does not contain any other point in  $P$  except its vertices.

Each tetrahedron is created with four Delaunay vertices. See figure 5 where a  $T_1$ ,  $T_2$  and two  $T_{12}$  tetrahedrons are translated from the Joint Voronoi Diagram in figure 4.

##### 3.1.1 Case 1: Voronoi Vertex Vs. Voronoi Edge

When five Delaunay vertices are co-spherical (Figure 6), a Voronoi vertex belonging to level  $i$  is exactly projected on a Voronoi edge belonging to level  $i+1$ , or vice versa (Figure 7).

The solution for such a degenerate condition is to pretend that  $VV_{123}$  is either above or below Voronoi edge  $VV_{ABD} \longleftrightarrow VV_{BCD}$ . For the first alternative, the virtual configuration appears in Figure 8, and its spatial consequence is displayed in Figure 9. For the second alternative, the virtual configuration is shown in Figure 10, while its spatial consequence is shown in Figure 11.

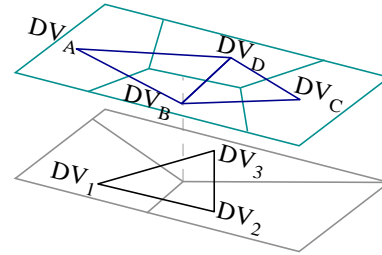


Figure 6: Voronoi vertex vs. Voronoi edge case. Vertices  $DV_1$ ,  $DV_2$ ,  $DV_3$ ,  $DV_B$  and  $DV_D$  are co-spherical.

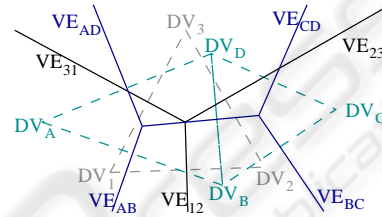


Figure 7: Voronoi vertex vs. Voronoi edge case. Joint Voronoi Diagram of levels  $i$  and  $i+1$ .

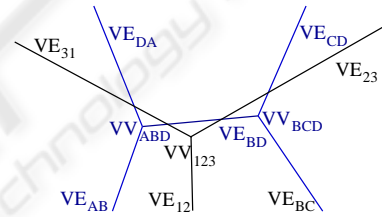


Figure 8: Voronoi vertex vs. Voronoi edge case. Delaunay vertex  $DV_D$  elected as apex.

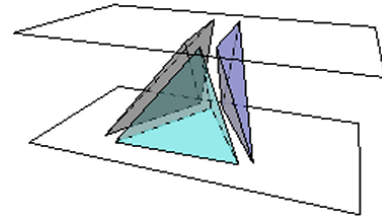


Figure 9: Voronoi vertex vs. Voronoi edge case. Spatial Configuration.

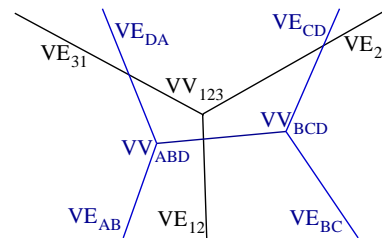


Figure 10: Voronoi vertex vs. Voronoi edge case. Delaunay vertex  $DV_B$  elected as apex.

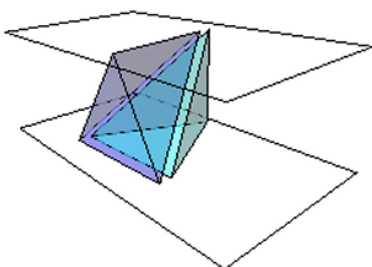


Figure 11: Voronoi vertex vs. Voronoi edge case. Delaunay vertex  $DV_B$  elected as apex.

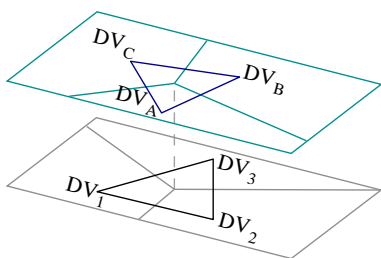


Figure 12: Voronoi Vertex vs. Voronoi Vertex case. Sub-case  $1a2b3c$ .

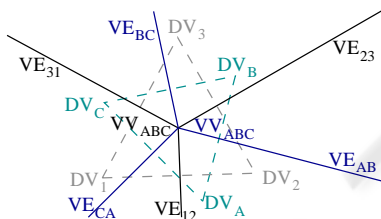


Figure 13: Voronoi Vertex vs. Voronoi Vertex case. Sub-case  $1a2b3c$ . Projection of Voronoi Diagrams of levels  $i$  and  $i + 1$ .

### 3.1.2 Case 2: Voronoi Vertex Vs. Voronoi Vertex

This case occurs when six Delaunay vertices are co-spherical. As a result, a Voronoi vertex of level  $i$  is projected onto a Voronoi vertex of level  $i + 1$ .

The sub-cases are determined by the distribution of the edges on the “intersecting star” created when all the edges are projected on the same plane (see figure 12 to 17 ). There are only two possible distributions. (a) the edges are intercalated or (b) they are not. When two consecutive edges belong to the same level, the sub-case is identified as the  $1ab23c$  sub-case. If there are no two consecutive levels belonging to the same level, the sub-case is identified as the  $1a2b3c$  one.

The sub-case  $1a2b3c$  appears in Figure 12. The Joint Voronoi Diagram for the levels  $i$  and  $i + 1$  appears in Figure 13. The virtual disturbance to solve this degeneracy appears in Figure 14, while its spatial effects do so in Figure 15.

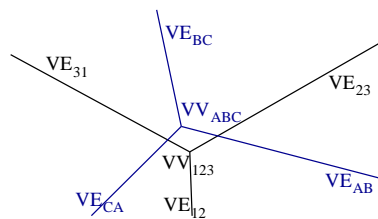


Figure 14: A virtual disturbance for the  $1a2b3c$  sub-case.

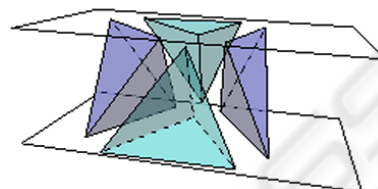


Figure 15: Spatial consequence for the virtual disturbance of Figure 14.

For the same situation, the sub-case  $1ab23c$  appears in Figure 16. For this case, the projection of the Voronoi Diagrams onto each other is seen in Figure 17. The virtual disturbances to solve this problem are shown in Figures 18, 19 and 20. A spatial configuration for one of such virtual scenarios appears in 21.

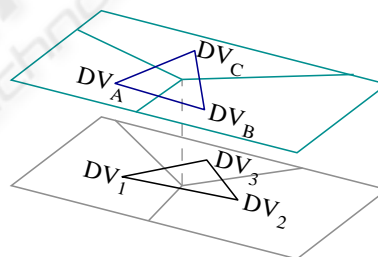


Figure 16: Voronoi Vertex vs. Voronoi Vertex case.  $1ab23c$  sub-case.

## 4 RESULTS

As said before, the special cases dealt with here are generated when more than four Delaunay vertices lie on the surface of an empty sphere. In the B+G method this situation leads to non-manifold surfaces, like the one shown in figure 22. The virtual perturbations proposed here avoid the uncertainty of the B+G method (which uses random numerical disturbances). Such virtual perturbations produce an improved result, shown in figure 23. Results for the Skull data set (figure 24) are shown in figure 25. The results for the data set *Brain* are shown in Figures 26 and 27. Other examples will be published in more extended reports of this investigation.

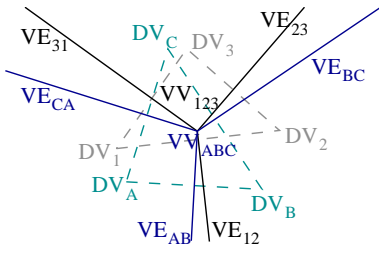


Figure 17: Voronoi Vertex vs. Voronoi Vertex case. *lab23c* sub-case.

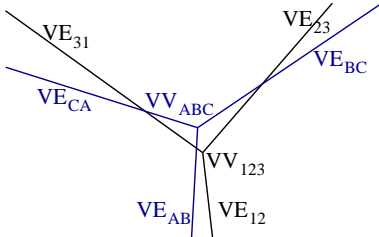


Figure 18: Virtual disturbance for the *lab23c* sub-case. Solution with three  $T_{12}$ .

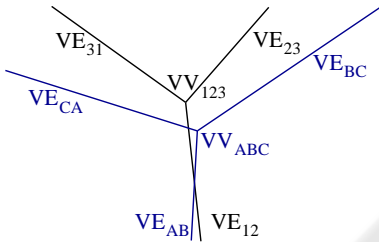


Figure 19: Virtual disturbance for the *lab23c* sub-case. Solution with two  $T_{12}$ .

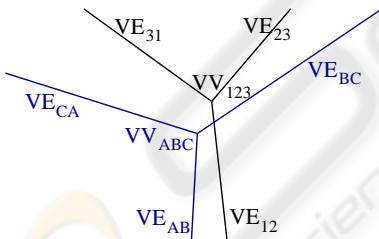


Figure 20: Virtual disturbance for the *lab23c* sub-case. Solution with just one  $T_{12}$ .

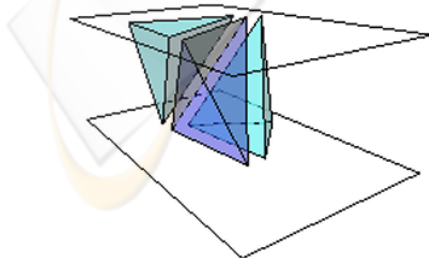


Figure 21: A spatial configuration for the *lab23c* sub-case.

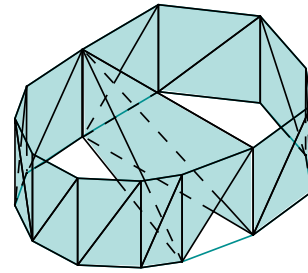


Figure 22: Surface reconstructed using the B+G method directly.

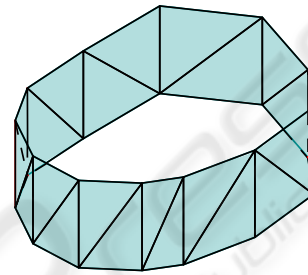


Figure 23: Surface reconstructed by the virtual disturbance method.



Figure 24: Detail of levels  $i$  and  $i+1$  of the set of contours "skull".

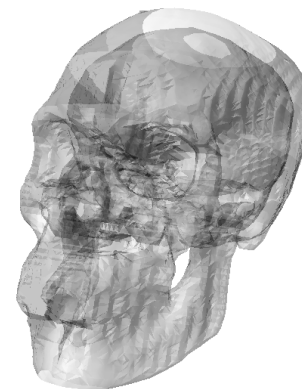


Figure 25: Reconstructed surface in a transparent material.



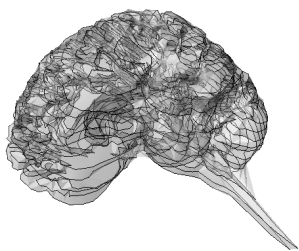


Figure 26: Set of contours.

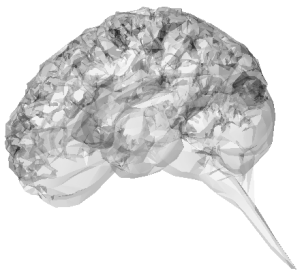


Figure 27: Reconstructed surface in a transparent material.

## 5 CONCLUSIONS

A method has been designed and implemented, to circumvent geometrical degeneracies arising from simultaneous processing of 2D superimposed Voronoi Diagrams, in the context of Surface Reconstruction from Slice Samples. In this particular problem, for each degenerate condition an enumerable finite set of non-degenerate counterparts is programmed, and instantiated as the geometry of the degeneracy dictates. In absence of the algorithm, self-intersecting and therefore non-manifold constructions are produced. With the algorithm, degenerate cases are mapped to their non-degenerate counterparts. This allows the normal downstream execution of the host algorithm (B+G, by Boissonnat & Geiger, 1988, 1993). The method presented classifies actions to be taken, based on the level of the degeneracy. The results show that the method is successful in removing the degeneracy, without further iterations and in a deterministic way. This method can be applied when the number of cases of degeneracy is known.

## REFERENCES

- Boissonnat, J. D. (1988). Shape reconstruction from planar cross-sections. *Computer Vision, Graphics and Image Processing*, pages 1–29.
- Burnikel, C., Fleischer, R., Mehlhorn, K., and Schirra, S. (1999). Efficient exact geometric computation made

easy. In *Proceedings of the 15th Annual ACM Symposium on Computational Geometry*.

- Edelsbrunner, H. and Mücke, E. P. (1990). Simulation of Simplicity: A technique to cope with degenerate cases in geometric algorithms. *ACM Transactions on Graphics*, 9(1):66–104.
- Funke, S., Klein, C., Mehlhorn, K., and Schmitt, S. (2005). Controlled perturbation for delaunay triangulations. In *Proceedings of S.O.D.A.*
- Geiger, B. (1993). Three dimensional modeling of human organs and its application to diagnosis and surgical planning. Research Report 2105, INRIA, Sophia-Antipolis, Valbonne, France.
- Ruiz, O., Cadavid, C., and Granados, M. (2002). Evaluation of 2d shape likeness for surface reconstruction. *Journal Anales de Ingenieria Grafica*, (15):16–24.
- Ruiz, O., Cadavid, C., Granados, M., Peña, S., and Vasquez, E. (2005). 2d shape similarity as a complement for voronoi-delaunay methods in shape reconstruction. *Elsevier Computer and Graphics*, 29(1):81–94.